Chemical Engineering Journal 98 (2004) 255–264

Chemical Engineering Journal

www.elsevier.com/locate/cej

Comparison of solutions for the homogeneous surface diffusion model applied to adsorption systems

Vinci K.C. Lee, Gordon McKay*

Department of Chemical Engineering, The Hong Kong University of Science and Technology, Clear Water Bay Road, Kowloon, Hong Kong, PR China

Accepted 15 August 2003

Abstract

Three solutions to the film surface diffusion mass transport model are discussed. The solutions are based on the homogenous surface diffusion model (HSDM) and are compared using three different adsorption systems. The mass transport solutions include a Crank–Nicholson implicit finite difference method, a semi-analytical solution method and a Cartesian collocation method. The three solutions are compared for accuracy, stability, convergence and computation CPU time.

The experimental systems used two adsorbents, activated carbon, a mainly microporous material, and sorbsil silica, a mainly macroporous material. Two categories of adsorbates were selected for the study, phenol, a relatively small organic molecule, which does not ionise, and basic dyes, larger organic structures, which exist as ionisable salts. A range of initial adsorbate concentrations were studied. The range of material types and experimental conditions selected should be sufficient to test and compare the three models under a variety of conditions.

Keywords: Adsorption systems; MMW model; WAMM model; Cartesian collocation model

1. Introduction

Adsorption may be defined as the removal of a component of a fluid by contacting the fluid with a solid adsorbent. Liquid-phase applications include the purification of drinking water, the removal of colour and harmful pollutants from wastewaters, the recovery of metals from ore leachates and the purification/separation of components in process streams [1–3]. Several types of contacting systems exist, such as, agitated batch, fixed beds and fluidised bed processes. The adsorption process is complex and considerable use is made of mathematical models to describe possible rate controlling mechanisms as well as computers to perform accurate and quick computation [4,5].

Three key steps are usually considered in adsorption processes in order to establish the rate controlling mechanism [6]:

(i) external mass transfer of the solute across the boundary layer of the particles;
(ii) adsorption at a specific surface site;
(iii) internal mass transfer within the particle by either (or both) a homogenous surface diffusion model (HSDM), or a pore diffusion model PDM within the liquid filled pores.

Step (ii) is generally assumed to be rapid and not involved in the rate controlling process.

The present paper compares the ability of a two resistance mass transfer model, based on external mass transfer and HSD, to predict concentration versus time decay curves for a number of agitated batch contact adsorption systems using three solutions for the HSDM, namely:

(i) Crank–Nicholson implicit finite difference method proposed by Mathews and Weber [7,8] has been modified to provide a more rapid solution and presented in this paper;
(ii) a semi-analytical integration formulation by McKay [9];
(iii) Cartesian collocation solution described by McKay [10].

The three solutions to the HSDM model are compared for accuracy, stability/convergence and CPU time.

Three experimental systems and sets of data were used for comparing the three models; these were the adsorption of phenol on activated carbon, the adsorption of basic yellow (Deorlene yellow) dye onto activated carbon and basic blue 69 (Astrazone blue) dye on sorbsil silica. Activated

* Corresponding author. Tel.: +852-2358-7133; fax: +852-2358-0054.
E-mail address: kemckayg@ust.hk (G. McKay).

1385-8947/$ – see front matter © 2004 Elsevier B.V. All rights reserved.
doi:10.1016/j.cej.2003.08.028

Nomenclature

a_R	Redlich–Peterson isotherm constant (dm^3/mg)
A_p	particle surface area (cm^2)
b_R	Redlich–Peterson isotherm constant (dm^3/g)
C	liquid-phase concentration at time t (mg/dm^3)
C_s	liquid-phase concentration at particle surface (mg/dm^3)
C_0	initial liquid-phase concentration (mg/dm^3)
d_p	mean particle diameter (μm, cm)
D	surface diffusion coefficient (cm^2/s)
j	assignment of individual jth exponential term equation
J_s	surface diffusion flux (mg/cm^2 s)
k_f	external mass transfer coefficient (cm/s)
n	number of experimental points
q	average solid-phase concentration in equilibrium with C_t (mg/g)
q_i	the concentration of solute inside a typical spherical at a distance r from the centre and at time t (mg/g)
q_r	solid-phase concentration at radial distance r within particle (mg/g)
q_s	solid-phase concentration at particle surface (mg/g)
r	radial distance from the centre of particle, $0 < r < R$ (cm)
R	radius of adsorbent particle (cm, μm)
t	time (s, min, h)
$u(x, \tau)$	transformed solid-phase concentration in homogenous solid-phase diffusion model ($=q(r/R)$)
V	liquid-phase volume (dm^3)
V_p	volume of adsorbent particle (cm^3)
W	weight of adsorbent (g)
x	dimensionless radius ($=r/R$)

Greek symbols

β	Redlich–Peterson isotherm constant
ε	particle voidage
$\lambda_{x,t}$	solution parameter ($=\Delta t/2(\Delta x)^2$)
λ_0	dimensionless empirical constant of λ for initial condition
ρ_p	apparent density of particle (g/cm^3)
τ	dimensionless time ($=(D_s t)/R^2$)

carbon comprises macropores, mesopores and an extensive microporous structure, whereas sorbsil silica has an extensive macropore structure with more limited micropore regions. The adsorbates selected for this study are phenol, a relatively small organic compound with some polar characteristics but no tendency to ionise; and, basic dyes which have an organic structure, are fairly larger molecular (molecular weight = 600–800 g/gmol) have a conjugate structure (to provide colour) and are salts which readily ionise in solution. Full details of the adsorbents, adsorbates, experimental methods and results have been reported previously for phenol/carbon [11], Deorlene yellow dye/carbon [12] and Astrazone blue dye/silica [13].

2. Theory

2.1. Development of equations

In the boundary layer, mass transfer is directly proportional to the difference in concentration of the solute in the bulk solution and that on the surface of the particle:

$$\text{rate} = k_f(C - C_s) \tag{1}$$

In homogenous surface diffusion the mass transfer of solute is by movement into the particle. For a spherical particle the equation describing the surface flux for this type of adsorption is defined [14,15] as

$$J_s = -\rho_p D \frac{dq_i}{dr} \tag{2}$$

The equation for boundary layer mass transfer in an agitated batch adsorber is

$$V_p \rho_p (1 - \varepsilon) \frac{dq}{dt} = \frac{k_f A_p (C - C_s)}{1000} \tag{3}$$

and by rearranging, this becomes

$$\frac{dq}{dt} = \frac{3k_f}{1000} \frac{C - C_s}{\rho_p (1 - \varepsilon) R} \tag{4}$$

The surface concentration, q_s is related to C_s, the equilibrium concentration in the liquid-phase at the surface of the particle, by the adsorption isotherm. Different forms of isotherm equation exist and in this study the following three-parameter equation, by Redlich and Peterson [16] is used to facilitate integration:

$$q_s = \frac{a_R C_s}{1 + b_R C_s^{\beta}} \tag{5}$$

The average concentration of solute in the particle q, is found by averaging the point concentration, q_i, over the volume of the particle:

$$q = 3 \int_0^r \frac{q_i r^2 \, dr}{R^3} \tag{6}$$

The concentration of solute inside a typical spherical particle at a distance r from the centre and at time t is denoted by $q_i(r, t)$. It is assumed that the internal mass transfer within the particle by a homogenous surface diffusion model (HSDM).

The HSDM was found to be applicable in these three adsorption systems [11–13]. The variation of q_i with distance and time is governed by the diffusion equation [17]:

$$\frac{\partial q_i}{\partial t} = D\left(\frac{\partial^2 q_i}{\partial r^2} + \frac{2}{r}\frac{\partial q_i}{\partial r}\right) \tag{7}$$

with the surface diffusion coefficient, D being constant.

The mass of solute diffusing across the boundary layer from the bulk solution in unit time is equal to the rate of build-up of solute in the adsorbent particle:

$$-V\frac{\mathrm{d}C}{\mathrm{d}t} = W\frac{\mathrm{d}q}{\mathrm{d}t} \tag{8}$$

Integrating,

$$\int_{C_n}^{C_{n+1}} \mathrm{d}C = -\frac{W}{V}\int_{q_n}^{q_{n+1}} \mathrm{d}q \tag{9}$$

$$C_{n+1} = C_n - \frac{W}{V}(q_{n+1} - q_n) \tag{10}$$

where n signifies any point in time.

Eqs. (7) and (8) are subject to the following initial and boundary conditions:

$$q_i(r, 0) = 0, \qquad C(0) = C_0 \tag{11}$$

$$q_i(R, t) = q_s(t) \tag{12}$$

2.2. Dimensionless form of the equations

Introducing the dimensionless variables τ and x for the independent variables t and r the equations become

$$\tau = \frac{Dt}{R^2} \tag{13}$$

$$x = \frac{r}{R} \tag{14}$$

and defining

$$u \equiv xq_i \tag{15}$$

Eqs. (3)–(11) become

$$\frac{\partial u}{\partial \tau} = \frac{\partial^2 u}{\partial x^2} \tag{16}$$

$$u(0, \tau) = 0 = u(x, 0) \tag{17}$$

$$u(1, \tau) = q_s(\tau) \tag{18}$$

$$q_s = \frac{a_R C_s}{1 + b_R C_s^{\beta}} \tag{19}$$

$$q(\tau) = 3\int_0^1 u(x, \tau)x\,\mathrm{d}x \tag{20}$$

$$\frac{\mathrm{d}q}{\mathrm{d}\tau} = \frac{3k_f R(C - C_s)}{D\rho_p(1 - \varepsilon) \times 1000} \tag{21}$$

$$C = C_0 - \left(\frac{W}{V}\right)q \tag{22}$$

The mathematical problem is the simultaneous solution of Eqs. (16)–(21).

2.2.1. Method 1—finite difference and the MMW model

Mathews and Weber [7,8], have proposed a scheme in which the diffusion equation (2) is solved using the Crank–Nicholson method which is based upon an implicit finite difference approximation.

This regime was programmed at the Queen's University of Belfast, by Madden [18], and by McCormak [19], who refined the model mathematically by incorporating a more accurate matrix method for solving the set of finite difference equations. The model is referred to as the MMW model, that is, the modified Mathews–Weber model. In the Crank–Nicholson scheme the diffusion equation (16) takes the form

$$\begin{aligned}&-\lambda_{x,\tau}u_{j+1}^{n+1} + (1 + 2\lambda_{x,\tau})u_j^{n+1} - \lambda_{x,\tau}u_{j-1}^{n+1}\\ &= \lambda_{x,\tau}u_{j+1}^{n} + (1 - 2\lambda_{x,\tau})u_j^{n} + \lambda_{x,\tau}u_{j-1}^{n}\end{aligned} \tag{23}$$

where $j = 2, M$ (distance steps) and $n = 1, N$ (time steps) and

$$\lambda_{x,\tau} = \frac{\Delta\tau}{2(\Delta x)^2} \tag{24}$$

From the initial and boundary conditions we have

$$u_1^n = 0 \quad \text{(center of the particle)} \tag{25}$$

$$u_j^1 = 0 \quad \text{(anywhere within the particle at } t = 0) \tag{26}$$

A similar expression is also derived for the surface boundary condition. The problem is to solve these equations subject to the specified boundary condition.

2.2.2. Method 2—integral formulation and the WAMM model

McKay [9] proposed a semi-analytical integral formulation solution of the diffusion equation (16). The starting point is a semi-analytical solution of the diffusion equation which satisfies the boundary condition equations (17) and (18):

$$\begin{aligned}u(x, \tau) = &\int_0^{\tau} \mathrm{d}\tau' f(\tau') \cdot 1\sqrt{(\tau - \tau')}\{\mathrm{e}^{-(x-1)^{**}2/4(\tau-\tau')}\\ &- \mathrm{e}^{-(x+1)^{**}2/4(\tau-\tau')}\}\end{aligned} \tag{27}$$

The following approximation is then derived:

$$u(x, \tau_n) \approx 3\sum_{j=1}^{n} f_i G_i(x, \tau_n) \tag{28}$$

where f_i is the average value of $f(\tau)$ in the interval τ_{i-1} to τ_i and

$$\begin{aligned}G_i(x, \tau_n) = &\int_{\tau_{i-1}}^{\tau_1} \mathrm{d}\tau' \frac{1}{(\tau_n - \tau)^{1/2}}\{\mathrm{e}^{-(x-1)^{**}2/4(\tau_n-\tau')}\\ &- \mathrm{e}^{-(x+1)^{**}2/4(\tau_n-\tau')}\}\end{aligned} \tag{29}$$

Similar approximations are then made for q of Eq. (20) and $\delta q/\delta\tau$ of Eq. (21). With suitable initial values for $q(\tau_0) = C_0$

it is the possible calculate values for these quantities at τ_1 and for q_s at τ_1. By repeating the cycle the quantities can be calculated at time τ_n.

The WAMM model was devised in response to the Mathews–Weber model being unable to handle a comprehensive range of physical systems and operating conditions because of deficiencies in the numerical solution of the diffusion equation. The model has been programmed, and provided a suitable time increment is chosen, this program gives stable predictions which closely agree with experimental results for wide range of operating conditions.

2.2.3. Method 3—collocation

The major objective of the present work is to solve the diffusion equation and hence the adsorption problem posed above Eqs. (16)–(22) using the method of collocation. As mentioned in the introduction the basis of the collocation method is to choose a trial solution for the differential equation under examination, which is consistent with the physical and mathematical constraints imposed by the problem. In orthogonal collocation the trial solution is expanded as a sum of products. One term of the product is an arbitrary constant/function which is to be determined. The other term is an orthogonal polynomial; the trial solution is therefore expanded in terms of orthogonal polynomials: the trial solution is therefore expanded in terms of orthogonal polynomials. These polynomials must also comply with the constraints of the problem.

In the present work it was decided to apply the method of Cartesian collocation. The method employed took as its trial solution the following integral:

$$u(x,\tau) = f(\tau)\{e^{-\lambda(1-x)^{**}2} - e^{-\lambda(1+x)^{**}2}\} \tag{30}$$

where $f(\tau)$ and $\lambda(\tau)$ are the average time functions to be determined. Since there are two unknowns two equations are required to solve for them. The first equation is obtained by substituting equation (30) into the diffusion equations:

$$\frac{\partial u}{\partial t} = f'\{e^{-\lambda(1-x)^2} - e^{-\lambda(1+x)^2}\} + f\{-(1-x)^2\lambda' e^{-\lambda(1-x)^2} + (1+x)^2\lambda' e^{-\lambda(1+x)^2}\} \tag{31}$$

$$\frac{\partial u}{\partial x} = f(\tau)\{2(1-x)\lambda e^{-\lambda(1-x)^2} + 2(1+x)\lambda e^{-\lambda(1+x)^2}\} \tag{32}$$

$$\frac{\partial u^2}{\partial x^2} = f\{-2\lambda e^{-\lambda(1-x)^2} + 2\lambda e^{-\lambda(1+x)^2} + 4(1-x)^2\lambda^2 e^{-\lambda(1-x)^2} - 4(1+x)^2\lambda^2 e^{-\lambda(1+x)^2}\} \tag{33}$$

The equation must be satisfied at some value $x = x$, x is the collocation point, x bar in the program, giving

$$f'\{e^{-\lambda(1-x')^2} - e^{-\lambda(1+x')^2}\} + f\lambda'\{-(1-x')^2 e^{-1(1-x')^2} + (1+x')^2 e^{-\lambda(1+x')^2}\} = 2f\lambda\{-e^{-\lambda(1-x')^2} + e^{-\lambda(1+x')^2} + 2(1-x')^2\lambda e^{-\lambda(1+x')^2} - 2(1+x')^2\lambda e^{-\lambda(1+x')^2}\} \tag{34}$$

For the second equation, the chemical engineering equations (20) and (21) are combined to give the condition:

$$\int_0^1 \frac{\partial u(x,t)}{\partial t} x\,dx = \frac{k_f R(C - C_s)}{D\rho_p(1-\varepsilon)\times 1000} \tag{35}$$

So,

$$f'\int_0^1 \{x e^{-\lambda(1-x)^2} - x e^{-\lambda(1+x)^2}\}\,dx + \lambda' f\int_0^1 \{-x(1-x)^2 e^{-\lambda(1+x)^2} + x(1+x)^2 e^{-\lambda(1+x)^2}\}\,dx = \frac{k_f R(C - C_s)}{D\rho_p(1-\varepsilon)\times 1000} \tag{36}$$

Some small initial time τ_1 is taken for the initial condition for Eqs. (34) and (36):

$$\lambda(\tau_1) = \frac{\lambda_0}{4\tau_1} \tag{37}$$

From the WAMM model it is expected for λ_0 to be a slowly varying function of τ_1, almost constant for sufficiently small τ_1.

The initial condition, $f(\tau_1)$ for Eqs. (36) and (37) is obtained from Eqs. (20) and (21) for sufficiently small τ_1:

$$f(\tau_1)\int_0^1 x\{e^{-\lambda(1-x)^2} - e^{-\lambda(1+x)^2}\}\,dx = \frac{\tau_1 k_f R C_0}{D\rho_p(1-\varepsilon)\times 1000} \tag{38}$$

The integral in Eq. (38) has been evaluated giving the error function:

$$f(\tau_1)\left\{\frac{\sqrt{\pi}}{2\sqrt{\lambda}}\mathrm{erf}(2\sqrt{\lambda}) - \frac{1}{2\lambda} + \frac{e^{-4\lambda}}{2\lambda}\right\} = \frac{\tau_1 k_f R C_0}{D\rho_p(1-\varepsilon)\times 1000} \tag{39}$$

where erf is the error function.

The ordinary differential equations (34) and (36) are solved simultaneously for $f(\tau)$ and $\lambda(\tau)$.

The boundary conditions for the surface concentration using Eqs. (17) and (18) become

$$q_s(\tau) = f(\tau)\{1 - e^{-4\lambda(\tau)}\} \tag{40}$$

Integration can now commence from $\tau = \tau_1$.

The objective is to determine values for q, the average concentration of solute in the adsorbent particle, C, the concentration of solute in the solution, and q_s and C_s, the surface concentrations in the solid- and liquid-phases, respectively.

Table 1
Model results for the adsorption of phenol on carbon ($C_0 = 47\,mg/dm^3$)

Time (min)	Concentration of phenol in solution (mg/dm^3)		
	Collocation	MMW	WAMM
0	47.00	47.00	47.00
10	40.34	40.48	40.48
20	35.02	35.26	35.26
30	30.74	31.00	31.00
40	27.30	27.28	27.48
50	24.54	24.54	24.54
60	22.31	22.08	22.08
70	20.54	20.00	20.00
80	19.10	18.24	18.24
90	17.75	16.74	16.74
100	17.02	15.45	15.46
110	16.28	14.35	14.36
120	15.66	13.41	13.41

Table 2
Model results for the adsorption of phenol on carbon ($C_0 = 100\,mg/dm^3$)

Time (min)	Concentration of phenol in solution (mg/dm^3)		
	Collocation	MMW	WAMM
0	100.00	100.00	100.00
10	85.84	86.09	86.31
20	74.54	75.45	75.77
30	65.50	67.13	67.48
40	58.27	60.48	60.83
50	52.50	55.08	55.40
60	47.89	50.61	50.91
70	44.21	46.87	46.97
80	41.27	43.55	43.95
90	38.93	40.98	41.22
100	37.07	38.65	38.87
110	35.58	36.62	36.83
120	34.35	34.86	35.05

3. Results and discussion

The three solution procedures described by methods 1–3 have been tested and compared using three adsorption systems, namely:

- phenol and activated carbon;
- Deorlene yellow (basic yellow 21 dye) on carbon;
- Astrazone blue (basic blue 69 dye) on silica.

The three systems were selected carefully. The adsorption of phenol onto activated is the system most frequently reported in the literature and involves the adsorption of a relatively small organic molecule onto the most widely used adsorbent, namely, activated carbon. The experimental data used for the correlations was that produced by Mathews and Weber [7,8]. The adsorption of basic yellow 21 dye onto carbon represents the adsorption of a larger more polar 'organic' molecule onto activated carbon. Its path or tortuosity through the extensive marco/microporous network in carbon would be more complex than that of the phenol molecule. The third system uses a basic dye but this time the

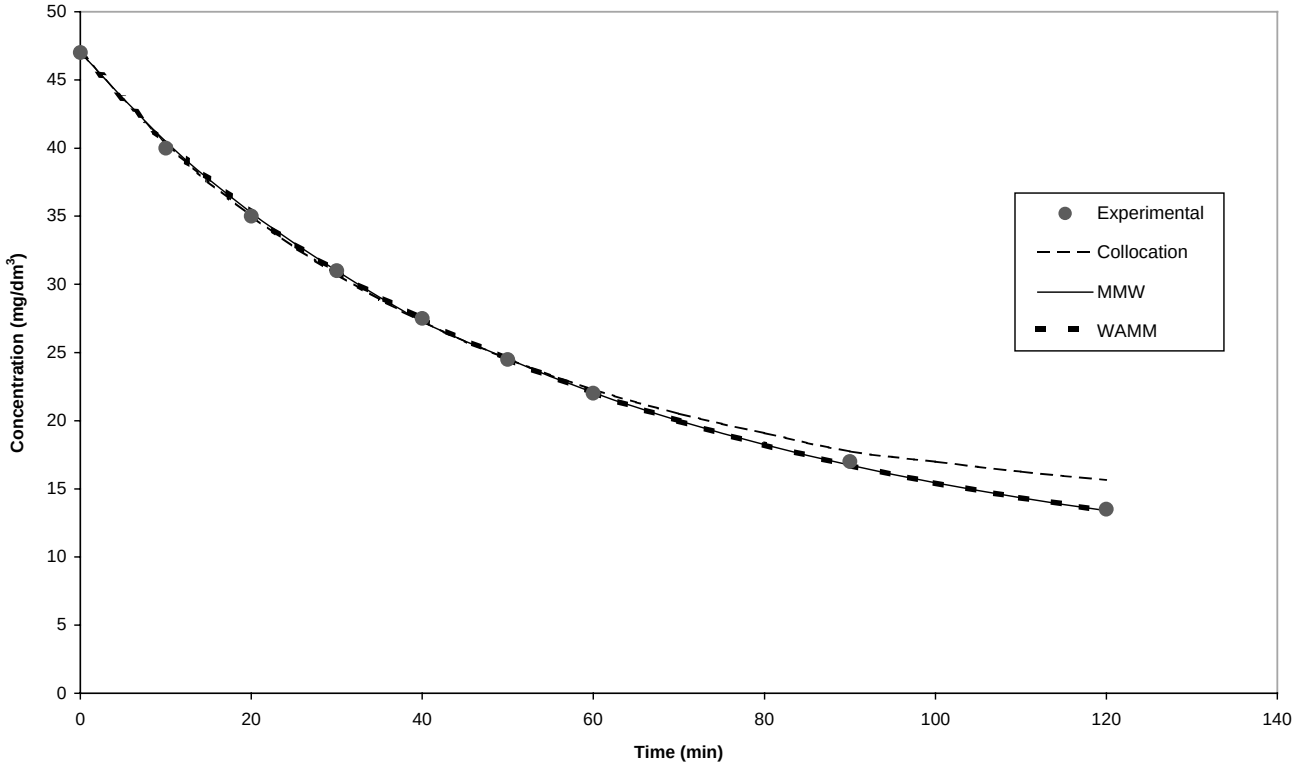

Fig. 1. The concentration decay curves using the three models in phenol/carbon system ($C_0 = 47\,mg/dm^3$).

Table 3
Adsorption of phenol on carbon (2 h run) ($C_0 = 47\,mg/dm^3$)

Dimensionless distance, x	Concentration of phenol in particle (mg/g)		
	Collocation	MMW	WAMM
0.0	0.000E+00	0.0000	0.0000
0.1	9.498E−18	0.2037	0.1958
0.2	9.529E−14	0.5844	0.5652
0.3	3.233E−10	1.400	1.362
0.4	3.712E−07	3.056	2.992
0.5	1.441E−04	6.156	6.061
0.6	1.893E−02	11.47	11.34
0.7	8.410E−01	19.80	19.65
0.8	1.263E+01	31.72	31.56
0.9	6.424E+01	47.16	47.05
1.0	1.1046E+02	65.31	65.27

Note. For collocation, the integration start time, $\tau_1 = 6$ min, the collocation point is 0.9 and the λ_0 is 3.9. Particle concentration profile from 0 to 60 min.

Table 4
Adsorption of basic yellow 21 on carbon ($C_0 = 100\,mg/dm^3$)

Time (min)	Concentration of dye in solution (mg/dm^3)		
	Collocation	MMW	WAMM
0	100.00	100.00	100.00
10	90.93	91.31	91.34
20	83.00	84.12	84.18
30	75.79	78.52	78.59
40	69.33	74.01	74.10
50	63.57	70.19	70.26
60	58.47	66.85	66.91
70	54.00	63.86	63.91
80	50.09	61.14	61.18
90	46.68	58.64	58.67
100	43.70	56.31	56.35
110	41.08	54.14	54.18
120	38.77	52.11	52.14

adsorbent is silica, a porous adsorbent, whose microporous network is not as complex and tortuous as that of carbon.

For all the tests, the data supplied to the collocation model were identical to that supplied to the WAMM (semi-analytical solution) and MMW (Crank–Nicholson finite difference) models.

The following test categories were studied:

1. the variation of solute concentration, C, with time;

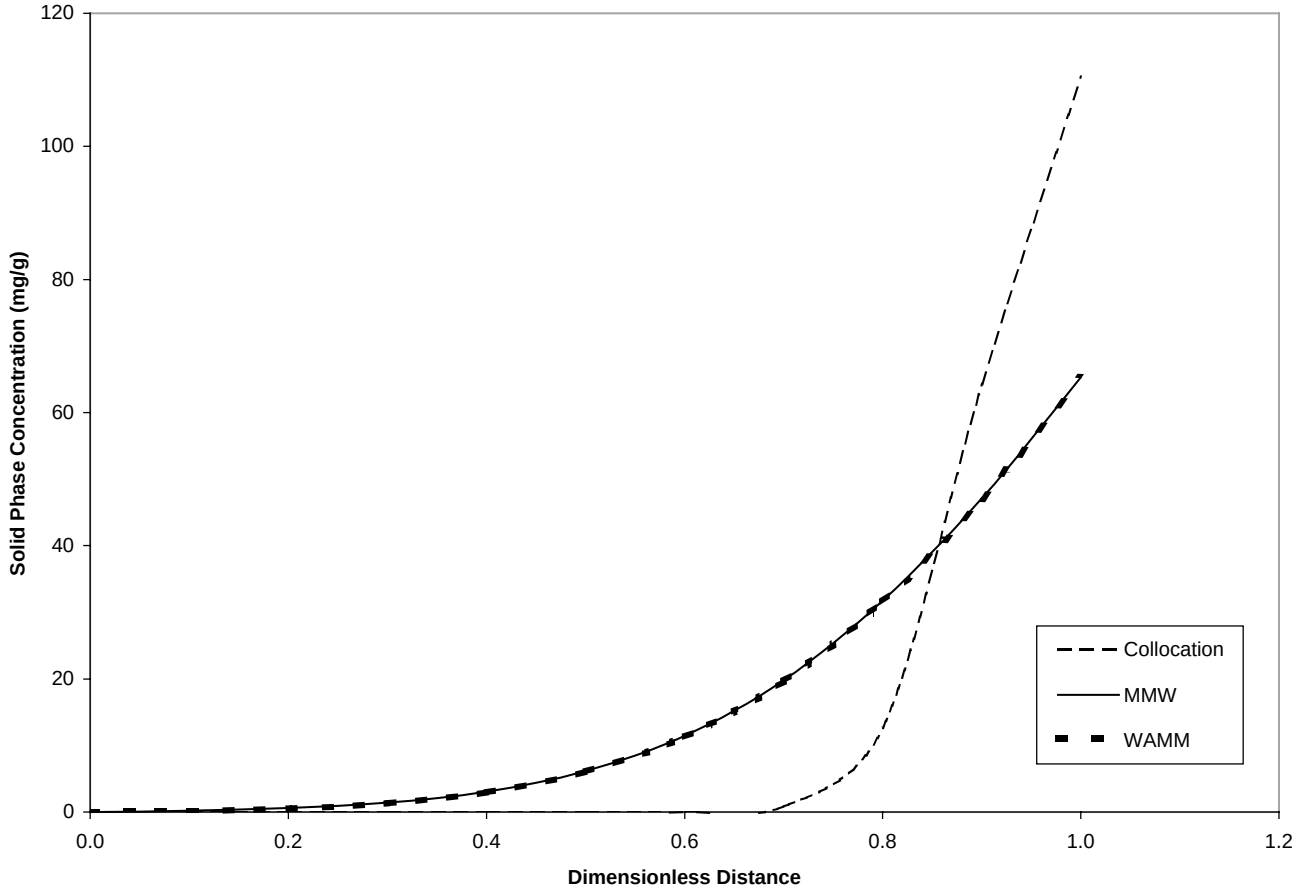

Fig. 2. The solid-phase concentration for the three models against dimensionless distance x at 60 min adsorption time in phenol/carbon system ($C_0 = 47\,mg/dm^3$).

Table 5
Solution concentration, $C_0 = 200$, with time

Time (min)	Concentration of dye in solution (mg/dm^3)		
	Collocation	MMW	WAMM
0	200.0	200.0	200.0
10	182.9	185.3	185.5
20	169.8	177.7	177.8
30	160.6	172.1	172.2
40	153.6	167.5	167.6
50	148.0	163.5	163.6
60	143.2	160.0	160.0
70	139.1	156.8	156.8
80	135.2	153.8	153.8
90	131.8	151.0	151.1
100	128.8	148.4	148.5
110	126.6	146.0	146.0
120	123.4	143.6	143.7

Table 6
Adsorption of basic yellow 21 on carbon

Dimensionless distance, x	Concentration of dye in particle (mg/g)		
	Collocation	MMW	WAMM
0.0	0.0000	0.0000	0.0000
0.1	0.0000	0.0000	0.0000
0.2	0.0000	0.0000	0.0000
0.3	0.0000	2.82E−33	0.0000
0.4	1.57E−36	1.21E−25	0.0000
0.5	6.66E−25	1.17E−14	0.0000
0.6	2.17E−15	2.00E−12	0.0000
0.7	5.43E−08	4.32E−07	6.68E−08
0.8	1.05E−02	7.66E−03	5.02E−03
0.9	15.50	6.52	6.40
1.0	176.68	181.10	181.10

Particle concentration profile from 0 to 60 min (2 h run) (C_0 = 200 mg/dm^3).

2. the variation in the surface concentrations, q_s and C_s with time.

3.1. Phenol/carbon system

The results of the computer outputs for the three solutions are compared in Tables 1 and 2 for two initial phenol concentrations, $C_0 = 47$ and 100 mg/dm^3. The WAMM and MMW models gave almost identical outputs up to the 2 h contact times for the concentration decay curves. All the predicted data for these two models also correlated all the experimental data points to within ±5%. At the lower initial concentration the collocation method gave almost identical output up to 70 min but at the higher initial phenol concentration deviation occurred after 30 min. The concentration decay curves using the three models are shown in Fig. 1, compared with the experimental data points. The solid-phase concentration

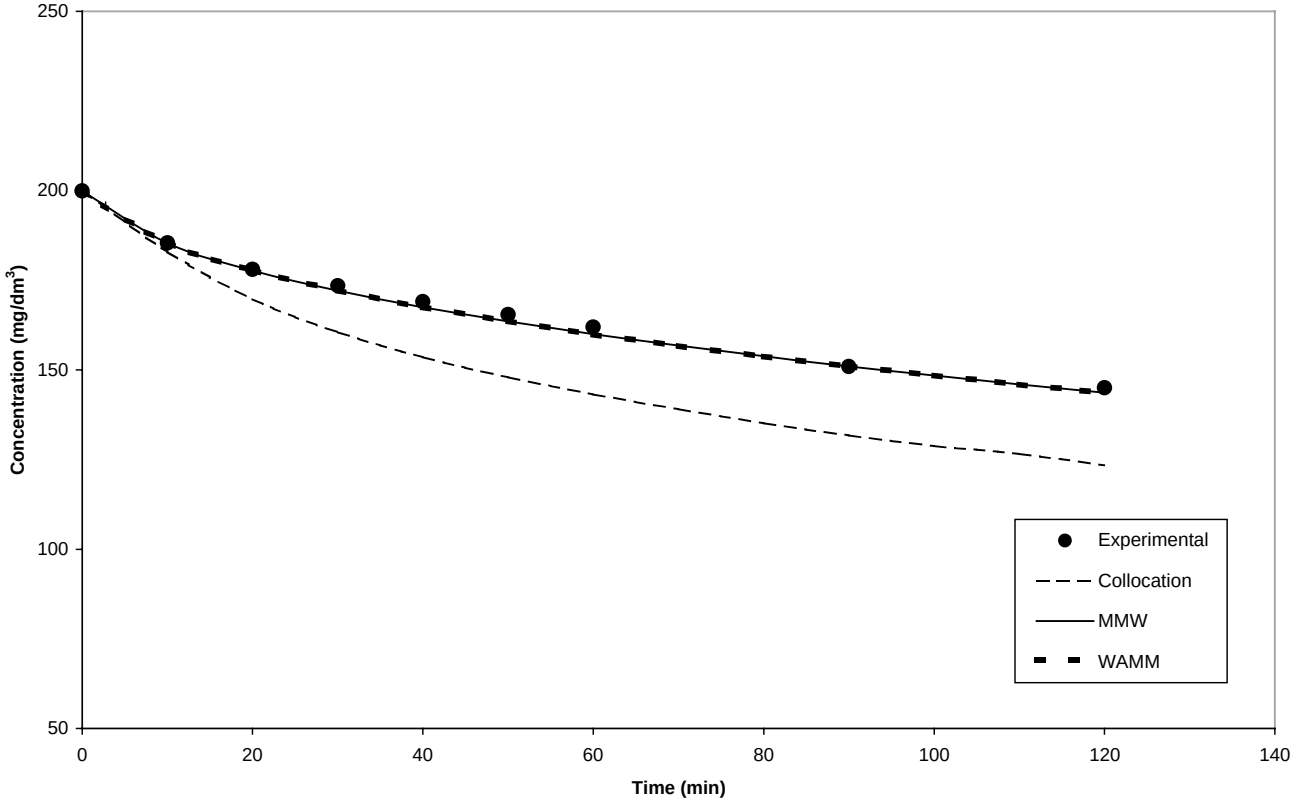

Fig. 3. The concentration decay curves using the three models in basic yellow 21/carbon system ($C_0 = 200$ mg/dm^3).

Table 7
Homogeneous surface diffusion (HSD) coefficients and external mass transfer coefficients (EMTC) for the systems

Systems	EMTC ($\times 10^{-6}$ m/s)	HSD coefficients ($\times 10^{-14}$ m^2/s)
Phenol/carbon	51	138
Basic yellow 21/carbon	10	3.0
Basic blue 69/silica	2.0	12.0

phenol distribution within the particle in terms of dimensionless distance, x, is shown in Table 3. Fig. 2 shows the solid-phase concentration for the three models against dimensionless distance $x(x = r/R)$ at 60 min adsorption time for the adsorption of phenol on carbon using an initial concentration of 47 mg phenol/dm^3.

3.2. Basic yellow 21/carbon system

The three solutions were compared using tow initial concentrations for basic yellow 21, namely, $C_0 = 100$ and 200 mg/dm^3, the results are shown in Tables 4 and 5, respectively. The outputs are compared in Fig. 3 for the initial dye concentration of 200 mg/dm^3. The WAMM and MMW data are almost identical and correlate the experimental data points. The theoretical points predicted by the collocation method for this system decay more rapidly than the experimental data and the other two models. After 40 min the deviation becomes greater than 10% and steadily increases with time. A more direct comparison can be made between the three models from Tables 4 and 5 and the trends are similar. The WAMM and MMW models give almost identical outputs and correlate experimental data almost exactly. The collocation model is not converging quickly enough. Table 6 shows the particle concentration profile at 60 min against dimensionless distance. At the surface, $x = 1.0$, the loading $q_{s(t=1)}$ is almost the same for the three models. Therefore, the problem does appear to be with convergence of the liquid concentration versus time decay profile. Consequently, in the case of phenol adsorption all three models generated very similar concentration versus time decay profiles, which agreed well with experimental data, the same trend was observed with basic yellow dye 21 on carbon. The difference in the chemistry of the system is principally that are dyes are more ionic in solution and are larger molecules. The differences result in significantly different surface diffusion coefficients as shown in Table 7, where D for phenol/carbon is 40 times greater than D for basic yellow 21/carbon.

3.3. Basic blue 69/silica system

The adsorption of Astrazone blue dye, that is, basic blue 69 onto the adsorbent Sorbsil silica has been studied. Silica is a more macroporous adsorbent than activated carbon, only requiring around 3.5 days to reach equilibrium [20], whereas phenol on carbon takes 4 weeks according to Peel et al. [21] and basic dyes on carbon up to 21 days according to McKay and Al Duri [22]. The effect of two initial dye concentrations, namely, $C_0 = 150$ and 200 mg/dm^3, have been studies. The three solutions to the HSDM are presented in Tables 8 and 9 for the initial dye concentrations of 150 and 200 mg/dm^3, respectively. In Table 8 the WAMM and collocation methods correlate experimental data points better than the MMW method. The experimental data points decay faster than the theoretical curve predicted by MMW solution method. The better quality of fit using the WAMM model can be seen in Fig. 4, which compares the three models with the experimental data points for the adsorption of basic yellow 21 dye onto activated carbon. This trend has been reported in previous work by McKay [9] and was the main reason for the development of the WAMM model. Consequently in this system the agreement in predicting concentration versus time decay curves accurately is between two different models from the basic yellow 21 dye on carbon. The differences in the system are mainly in the internal structure of the adsorbent in terms of surface area and porosity/pore size

Table 8
Adsorption of basic blue 69 on silica ($C_0 = 150$ mg/dm^3)

Time (min)	Concentration of dye in solution (mg/dm^3)		
	Collocation	MMW	WAMM
0	150.00	150.00	150.00
10	141.48	145.01	142.71
20	135.04	141.81	138.12
30	130.21	139.58	134.66
40	126.61	137.64	131.83
50	123.86	135.96	129.39
60	121.71	134.48	127.25
70	119.97	133.15	125.32
80	118.55	131.93	123.56
90	117.36	130.80	121.94
100	116.38	129.74	120.43
110	115.54	128.76	119.02
120	114.83	127.83	117.70

Table 9
Adsorption of basic blue 69 on carbon ($C_0 = 200$ mg/dm^3)

Time (min)	Concentration of dye in solution (mg/dm^3)		
	Collocation	MMW	WAMM
0	200.00	200.00	200.00
10	188.96	193.89	190.98
20	181.25	190.45	185.88
30	176.01	187.89	182.10
40	172.32	185.80	179.02
50	169.54	183.91	176.37
60	167.36	182.39	174.03
70	165.60	180.95	171.91
80	164.16	179.62	169.98
90	162.97	178.39	168.20
100	161.98	177.25	166.53
110	161.14	176.18	164.98
120	160.44	175.16	163.51

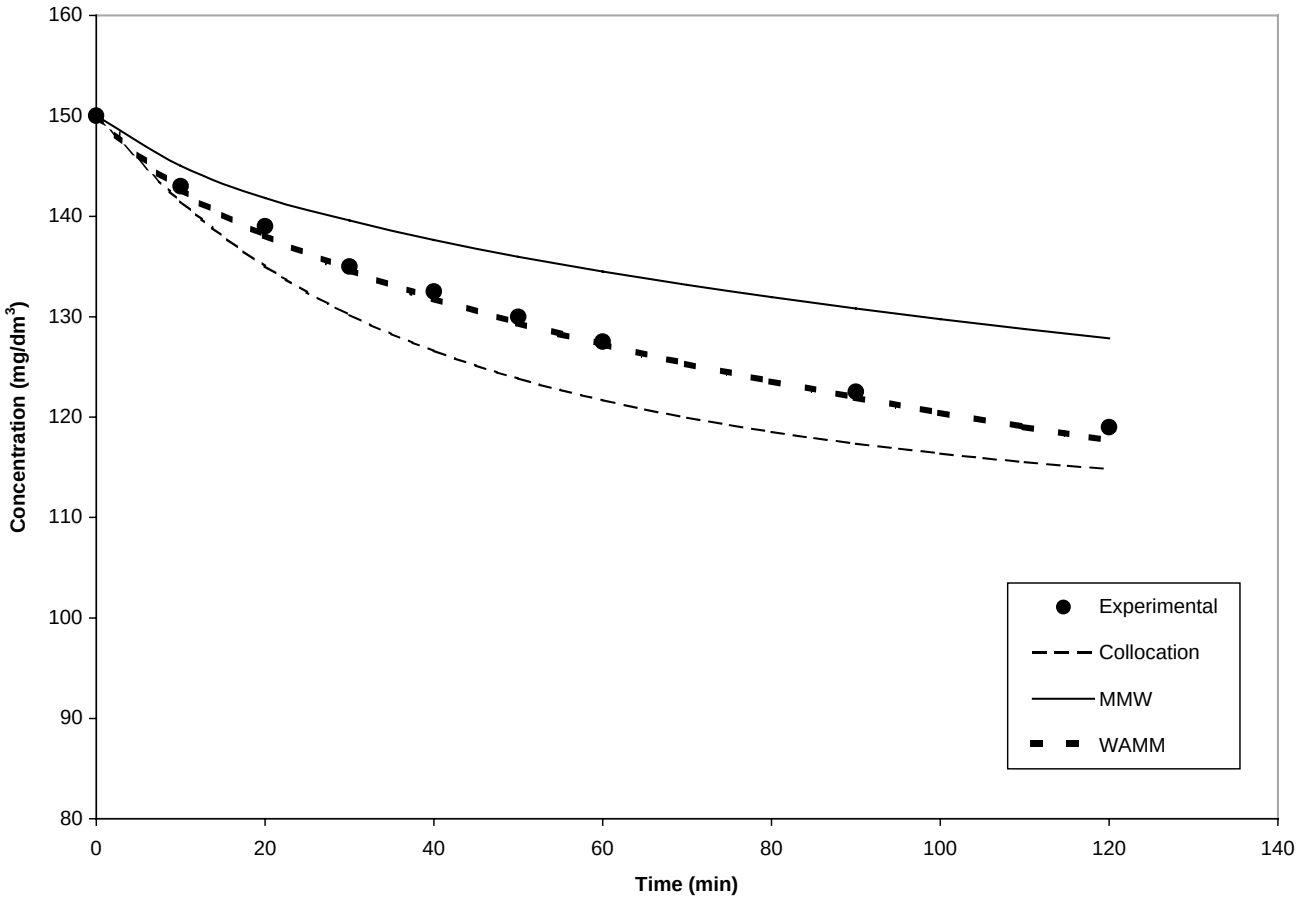

Fig. 4. The concentration decay curves using the three models in basic yellow 21/carbon system ($C_0 = 150\,mg/dm^3$).

distribution. The difference is shown by the D values; for basic blue 69 on silica D is four times greater than D for basic yellow 21 on carbon. The lower diffusivity for basic yellow 21 limits the rate at which the MMW solution model can diffuse the dye and predicts values higher than experimental data points. Nevertheless, all the theoretical data points from the three solutions are within 12% up to 2 h contact time.

3.4. CPU times

The results shown in Tables 1–9 were obtained by running the computer programmes to obtain convergence, that is, constant values of all concentration versus time relationships. Initially a set number of integration steps are specified for the 2 h contact time period and the programme is run. The number of integration steps is steadily increased until a constant output is obtained. The required time to achieve this output is referred to as the minimum CPU time. As the number of integration steps increases so does the minimum processing time. The relative CPU times to achieve the outputs in Tables 1–9 are presented in Table 10, using Fortran 77. The basis for the relative CPU is that the shortest processing time has been assigned an arbitrary value of 1000. This occurred using the WAMM model for the phenol/activated carbon system using an initial phenol concentration of $47\,mg/dm^3$. Table 10 shows the CPU times using the semi-analytical WAMM solution model are the lowest to achieve convergence of the programme. The WAMM solution model had difficulty in convergence when large molecules were being adsorbed and the surface diffusion coefficients were relatively low. The CPU times for the

Table 10
Relative CPU times

System name	Relative CPU time		
	Collocation	MMW	WAMM
Phenol/carbon, $C_0 = 47\,mg/dm^3$	5.019	1.650	1.000
Phenol/carbon, $C_0 = 100\,mg/dm^3$	5.137	1.653	1.010
Deorlene yellow/carbon, $C_0 = 100\,mg/dm^3$	4.727	46.10	1.481
Deorlene yellow/carbon, $C_0 = 200\,mg/dm^3$	4.252	46.48	1.465
Basic blue 69/silica, $C_0 = 150\,mg/dm^3$	3.578	21.12	1.011
Basic blue 69/silica, $C_0 = 200\,mg/dm^3$	3.588	21.38	1.029

collocation model were relatively constant but agreement with experimental data was not very good for one system, namely, the adsorption of basic yellow 21 onto carbon.

3.5. Solution stability

Stability was taken to have been achieved when results for two integration ranges (specified by the number of integration time steps) differed by no more than 1%. Although stability was observed outside this range the error increased significantly as the number of integration time steps was decreased or increased. For the MMW model, the solution concentration value remained relatively stable for the number of integration time steps in the range 100–2400. For the WAMM model, it remained very stable when the number of integration steps falls between 100 and 3000. Therefore, the WAMM and MMW both gave stable solutions for a large range of the number of integration time steps.

The solution concentrations for the collocation model are reasonably close to the WAMM values. On average they tend to be below the WAMM model values whereas those predicted by the MMW model tend to be above the WAMM values. Particle concentration profiles as predicted by collocation and the WAMM model are often zero for a large part of the adsorbent particles' radius. In the case of collocation this occurs because the concentration is given by Eq. (30) and is dependent on $f(\tau)$ and $\lambda(\tau)$, and is coupled with rounding errors and finite machine accuracy (which are also applicable to the WAMM and MMW models); this is also important for values near centre of the particle which are small and more prone to these limitations. The value calculated for q_s from the boundary condition, Eq. (29) is highly dependent on $\lambda(\tau)$ and the term containing $\lambda(\tau)$ becomes effectively zero for large values of $\lambda(\tau)$. For some operating conditions of the system, such as basic yellow/carbon, it was observed that q_s first dropped and then increased. Therefore, there are more factors to affect the stability of the solution using a collocation model than that in WAMM and MMW models.

4. Conclusions

On the basis of the data presented in this paper and using computer programmes of a similar structure for the three solution methods, the semi-analytical model seems the most effective and efficient in terms of processing time and accuracy. However, only three experimental systems have been tested using two sets of data for each system, observations based on such limited applications may not be conclusive. The solution concentrations for the collocations solution model are reasonably close to the WAMM solution model and in excellent agreement of the phenol/carbon system and basic blue 69/silica system. More effective processing times may be available if multiple point or orthogonal collocation solutions were used. These need to be developed and tested. Furthermore, the solution methods based on multipoint collocation developed by Tien [4,23] should be tested and compared with the present models.

References

[1] G. McKay, Use of Adsorbents for the Removal of Pollutants form Wastewaters, CRC Press, London, 1995.
[2] G. McKay, S.J. Allen, Low cost adsorbents in continuous processes, in: D.A.I. Wase, C.F. Forster (Eds.), Biosorbents for Metal Ions, Taylor & Francis, London, 1997 (Chapter 9).
[3] B. Volesky, Z.R. Holan, Review: biosorption of heavy metals, Biotechnol. Progr. 11 (1995) 235–250.
[4] C. Tien, Adsorption Calculations and Modelling, Butterworths/Heinnemann, London, 1994.
[5] D.D. Do, Adsorption Analysis: Equilibrium and Kinetics, Imperial College Press, UK, 1998.
[6] T. Furusawa, J.M. Smith, AIChE J. 19 (1973) 401–408.
[7] A.P. Mathews, W.J. Weber Jr., Effects of external mass transfer and intraparticle diffusion on adsorption rates in slurry reactors, AIChE Symp. Ser. 73 (166) (1976) 91–98.
[8] A.P. Mathews, W.J. Weber Jr., Modeling and parameter evaluation for adsorption in slurry reactors, Chem. Eng. Commun. 25 (1984) 157–171.
[9] G. McKay, Application of surface diffusion model to the adsorption of dyes on bagasse pith, Adsorption 4 (1998) 361–372.
[10] G. McKay, Solution to the homogenous surface diffusion model for batch adsorption systems using orthogonal collocation, Chem. Eng. J. 81 (2001) 213–221.
[11] G. McKay, M.J. Bino, R. Altamemi, The adsorption of various pollutants from aqueous solutions on to activated carbon, Water Res. 19 (4) (1985) 491–495.
[12] G. McKay, The adsorption of dyestuffs from aqueous solutions using activated carbon. IV. Intraparticle diffusion processes, J. Chem. Technol. Biotechnol. 33A (1983) 205–218.
[13] G. McKay, M.S. Otterburn, A.G. Sweeney, The removal of colour from effluents using various adsorbents. III. Silica: rate processes, Water Res. 14 (1980) 15–20.
[14] S. Masamune, J.M. Smith, AIChE J. 10 (1964) 246–254.
[15] S. Masamune, J.M. Smith, Adsorption rate studies: interaction of diffusion and surface processes, AIChE J. 11 (1965) 34.
[16] O. Redlich, D.L. Peterson, A useful adsorption isotherm, J. Phys. Chem. 63 (1959) 1024.
[17] J. Crank, The Mathematics of Diffusion, 2nd ed., Clarendon Press, Oxford, 1975.
[18] J.A. Madden, Development of programs for diffusional mass transfer processes, MSc Thesis, The Queen's University of Belfast, 1983.
[19] S.C. McCormak, Comparison and development of mathematical models for the adsorption of pollutants from solutions, MSc Thesis, The Queen's University of Belfast, 1984.
[20] G. McKay, The adsorption of basic dye onto silica from aqueous solution–solid diffusion model, Chem. Eng. Sci. 39 (1984) 129–138.
[21] R.G. Peel, A. Benedek, C.M. Crowe, A branched pore kinetic model for activated carbon, AIChE J. 27 (1981) 26–34.
[22] G. McKay, B.A. Al Duri, Branched-pore model applied to the adsorption of basic dyes on carbon, Chem. Eng. Process. 24 (1988) 1–14.
[23] C. Tien, Adsorption kinetics of a nonflow system with nonlinear equilibrium relationship, AIChE J. 7 (1961) 410–416.